Fungal Biology 130 (2026) 101824

Contents lists available at ScienceDirect

Fungal Biology

journal homepage: www.elsevier.com/locate/funbio

Developmental stage-dependent and wound-triggered formation dynamics of volatiles in *Pleurotus cornucopiae*

Yuki Nagata [a], Kozue Sotome [b], Daisuke Fukuyama [c], Kanako Sekimoto [c], Kenji Matsui [a,*]

[a] Graduate School of Sciences and Technology for Innovation (Agriculture), Yamaguchi University, Yamaguchi, 753-8515, Japan
[b] Fungus/Mushroom Resource and Research Center, Faculty of Agriculture, Tottori University, Tottori, 680-8553, Japan
[c] Graduate School of Nanobioscience, Yokohama City University, Yokohama, 236-0027, Japan

ARTICLE INFO

Keywords:
Pleurotus cornucopiae
Volatile organic compounds
C8 oxylipins
Wound-induced volatiles
PTR-ToF-MS

ABSTRACT

Volatile organic compounds (VOCs) emitted by fungi play crucial roles in ecological interactions, including spore dispersal, defense, and communication with other organisms. However, developmental regulation and biosynthetic relationships among individual fungal VOCs remain poorly understood. In this study, we investigated growth-stage-dependent and wound-induced VOC emissions in the basidiomycete *Pleurotus cornucopiae* by combining nondestructive headspace sampling, GC–MS analysis, controlled wounding and feeding experiments, and real-time monitoring using proton-transfer-reaction time-of-flight mass spectrometry (PTR-ToF-MS). Developmental profiling revealed distinct emission patterns of fatty-acid-derived oxylipins and sesquiterpenes, with sesquiterpenes accumulating predominantly during the late fruiting body stages associated with spore release, whereas eight-carbon (C8) VOCs were transiently enhanced during the early reproductive stages. Mechanical wounding triggered an immediate burst of C8 VOCs including 1-octen-3-ol, 1-octen-3-one, and 3-octanone. PTR-ToF-MS analysis resolved their production kinetics at second-scale resolution, demonstrating the nearly simultaneous formation of 1-octen-3-ol and 1-octen-3-one, followed by delayed accumulation of 3-octanone. Cell-free enzyme assays indicated that enzymatic cleavage of linoleic acid 10(*S*)-hydroperoxide predominantly yielded 1-octen-3-ol. Feeding experiments and tissue disruption analyses further suggested that 3-octanone formation requires metabolic cooperation between damaged and adjacent intact tissues. Taken together, these results indicated that *P. cornucopiae* controls VOC production in a growth-and damage–dependent manner. We hope that our findings will facilitate future investigations on the ecological and physiological roles of dynamic VOC regulation during mushroom fruiting body development and in response to wounding.

1. Introduction

Volatile organic compounds (VOCs) emitted by fungi play important roles in ecological interactions, including communication with fungivores, defense against antagonists, and interactions with other microorganisms (Inamdar et al., 2020). Basidiomycetous fungi release characteristic VOC blends that change dynamically during development and in response to mechanical damage (Combet et al., 2009; Fäldt et al., 1999; Orban et al., 2020). Among fungal VOCs, eight-carbon (C8) VOCs, including 1-octen-3-ol, 1-octen-3-one, and 3-octanone, are ubiquitous and abundant, whereas sesquiterpenes constitute an important and often substantial fraction of the VOC blends emitted by fungi (Fäldt et al., 1999; Orban et al., 2020). 1-Octen-3-ol, often referred to as "mushroom alcohol," is produced by most ascomycetes and basidiomycetes and has been detected even in bryophytes and some angiosperms (Pennerman et al., 2022). It has been proposed that 1-octen-3-ol in basidiomycetous fungi is generated from linoleic acid via oxygenation to linoleic acid 10(*S*)-hydroperoxide (10(*S*)HPODE), followed by cleavage of this hydroperoxide (Wurzenberger and Grosch, 1984). In parallel, various sesquiterpenes derived from the mevalonate pathway are emitted in species-, tissue-, and development-dependent manners, presumably contributing to both the ecological interactions and characteristic aromas of fruiting bodies (Orban et al., 2023; Wang et al., 2021). Despite this general framework, the regulation of C8 VOCs and sesquiterpene biosynthesis, and its relationship with the respective physiological and ecological functions of these VOCs, remain poorly

* Corresponding author. Graduate School of Sciences and Technology for Innovation (Agriculture), Yamaguchi University, Yoshida 1677-1, Yamaguchi City, Yamaguchi, 753-8515, Japan.
E-mail address: matsui@yamaguchi-u.ac.jp (K. Matsui).

https://doi.org/10.1016/j.funbio.2026.101824
Received 23 February 2026; Received in revised form 15 July 2026; Accepted 16 July 2026
Available online 17 July 2026
1878-6146/© 2026 The Authors. Published by Elsevier Ltd on behalf of British Mycological Society. This is an open access article under the CC BY license (http://creativecommons.org/licenses/by/4.0/).

understood.

Mechanical damage to fungal tissues triggers a rapid and massive burst of C8 VOCs, and this wound-induced response is thought to be of ecological significance (Combet et al., 2009; Fäldt et al., 1999; Inamdar et al., 2020; Orban et al., 2020). Despite this presumed ecological relevance, most studies have relied on endpoint analyses with limited temporal resolution, making it difficult to resolve precursor–product relationships among individual C8 VOCs and to elucidate their distinct production dynamics at high temporal resolution. In contrast, real-time monitoring using proton-transfer-reaction mass spectrometry (PTR-MS) was instrumental in establishing the biosynthetic sequence of green leaf volatiles (GLVs) in angiosperms, demonstrating that (*Z*)-3-hexenal is rapidly reduced to (*Z*)-3-hexen-1-ol and subsequently acetylated to (*Z*)-3-hexen-1-yl acetate (D'Auria et al., 2007). Although PTR-MS has been applied to fungal VOC analysis (Aprea et al., 2015; Chang and Urban, 2018), such studies remain relatively scarce, and its potential for dissecting rapid wound-induced VOC formation in fungi has not been fully exploited. In addition to biosynthetic relationships, the cellular context of VOC formation is an important but largely unexplored aspect of fungal C8 VOC metabolism. In plants, wound-induced GLV biosynthesis depends on enzyme activation in damaged cells and metabolic cooperation between damaged and adjacent intact cells (Matsui et al., 2012). Whether a similar tissue-level coordination is required for C8 VOC formation in fungi remains unknown.

In this study, we investigated the developmental and wound-induced emissions of VOCs in the basidiomycete *Pleurotus cornucopiae* (golden oyster mushroom). *P. cornucopiae* was selected as a model basidiomycete because its cultivation period is notably shorter (16–30 days) than that of other commercially cultivated mushrooms, and its mycelial growth and fruiting body formation can be efficiently reproduced under laboratory conditions, allowing precise experimental control of the developmental stage and tissue damage. Furthermore, *P. cornucopiae* var. *citrinopileatus* was recently reported as an invasive species in North America, where it disrupts native fungal communities (Veerabahu et al., 2025). VOC-mediated chemical-ecological interactions have been suggested as factors contributing to ecological competitiveness. Moreover, *P. cornucopiae* is regarded as a promising edible mushroom containing bioactive compounds with potential health benefits, such as ergothioneine (Sato et al., 2025), thereby making insights into VOC biosynthesis relevant to both fundamental research and future food-related applications. By combining nondestructive VOC sampling during fruiting body development, GC–MS quantification, controlled wounding and feeding experiments, and real-time PTR– time-of-flight (ToF)–MS analysis, we aimed to (i) characterize growth stage–dependent VOC emission profiles, (ii) resolve the temporal dynamics of wound-induced C8 compounds, and (iii) examine how tissue integrity influences the production ratios of C8 compounds. Our results provide new insights into the regulation, potential functions, and biosynthesis of VOCs in the fruiting bodies of mushrooms.

2. Materials and methods

2.1. Fungal strain and culture conditions

P. cornucopiae strain TUFC 33027 was obtained from the Fungus/Mushroom Resource and Research Center (FMRC), Tottori University Fungal Culture (TUFC), with support from the National BioResource Project of MEXT, Japan. The strain was maintained on malt extract agar (MA) (Shimadzu Diagnostics Co., Tokyo, Japan) plates at 25 °C in the dark. For cultivation, a substrate consisting of oak sawdust and rice bran (3:1, v/v) was prepared, and tap water was added to adjust the moisture content to approximately 65% of the dry weight of the substrate. The substrate (300 g per bag) was packed into filter-equipped polyethylene cultivation bags (S-25ES; Sakato Sangyo Co., Ltd., Gunma, Japan), heat-sealed, and autoclaved to prepare the mushroom beds. Mycelia grown on MA plates for 2 weeks were excised together with the agar using a sterile scalpel and inoculated onto sterilized mushroom beds. After inoculation, the bags were resealed and incubated at 22 °C under weak light (1 μmol m^{-2} s^{-1}) with a 14 h light/10 h dark photoperiod. In this study, this growth stage was designated MoB (mycelia on the mushroom bed), followed by the number of days after inoculation. After 2 weeks, the substrate was fully colonized by mycelia, hereafter referred to as the fully colonized mycelium (FCM). The upper surface of the bags was then removed, and cultivation was continued at 22 °C and 70% relative humidity under fluorescent light (48 μmol m^{-2} s^{-1}) with a 14 h light/10 h dark photoperiod. During this period, water was sprayed twice daily (approximately 3.5 mL per bed) to maintain adequate surface moisture. After primordium formation, cultivation continued for an additional week, and this stage was designated as FB (fruiting body).

2.2. VOC collection and analysis

The mushroom bed was placed in a 1 L separable flask, and air was continuously supplied at flow rates of 0.3 L min^{-1} at the inlet and 0.2 L min^{-1} at the outlet (Supplementary Fig. S1). One mushroom bed was placed in a separable flask, and three independent flask sets were prepared as biological replicates for VOC collection ($n = 3$). After purging the system for 30 min without an adsorbent, a Tenax TA adsorbent (180 mg, 60/80 mesh; CAMSCO, Tokyo, Japan) was installed, and VOCs were collected for 90 min. After VOC collection, the mushrooms were returned to the growth chamber. VOC sampling was conducted between 9:30 and 11:00 JST and 15:30 and 17:00 JST. As the lights were turned on at 08:00, these sampling periods corresponded to 1.5–3 h and 7.5–9 h after light onset, respectively. Prior to analysis, 1 μL of an acetone solution containing *n*-nonanyl acetate (1 μg $μL^{-1}$; Tokyo Chemical Industry, Tokyo, Japan) was added as an internal standard using a microsyringe. The internal standard was drawn through the adsorbent using an automated gas-sampling pump (GSP-300FT-2; Gastec Co., Kanagawa, Japan) at 100 mL min^{-1} for 5 min. VOCs were analyzed using thermal desorption–gas chromatography–MS (TD–GC–MS) using a GC-MS-TQ8040 NX system coupled with a TD-30 thermal desorption unit (Shimadzu Corp., Kyoto, Japan). VOCs were desorbed at 250 °C for 10 min with helium as the carrier gas at 70 mL min^{-1}. The analytes were cryofocused at −25 °C in a cold trap and subsequently transferred to the GC column (InterCap WAX, 30 m × 0.25 mm i.d., film thickness 0.25 μm; GL Sciences Inc., Tokyo, Japan) by rapid heating of the trap to 250 °C. The GC oven temperature program was as follows: 40 °C for 5 min; 40–200 °C at 5 °C min^{-1}; and 200 °C for 5 min. Helium was used as a carrier gas at a constant pressure of 86.1 kPa. The mass spectrometer was operated in electron ionization (EI) mode at 70 eV, with an ion source temperature of 200 °C. The retention index of each peak was calculated using a C8–C20 alkane mixture (Sigma–Aldrich, St. Louis, MO, USA). Authentic standards of 1-octen-3-ol (Tokyo Chemical Industry), 3-octanone (FUJIFILM Wako Pure Chemical Corp., Osaka, Japan), 1-octen-3-one (Tokyo Chemical Industry), δ-cadinene (Tokyo Chemical Industry), and α-copaene (Toronto Research Chemicals, Toronto, ON, Canada) were used for peak assignment. The retention indices and mass spectra of α-muurolene, γ-muurolene, and τ-cadinol were verified and corrected using hinoki cypress (*Chamaecyparis obtusa*) wood pellets (Coona Co., Kanagawa, Japan) (Matsui et al., 2007). Other compounds were tentatively identified by comparison with the NIST Mass Spectral Library (version 17s) using GCMSsolution software (Shimadzu) and by comparing their RI values with those reported in the NIST database (https://webbook.nist.gov/chemistry/). Compounds exhibiting less than 90% similarity to the NIST library were designated as sesquiterpenes (1) – (3) when their mass spectral profiles clearly indicated sesquiterpene structures. The RI values and identification criteria for each compound are summarized in Supplementary Table S1. A heatmap was generated to visualize the changes in VOC emission profiles during mushroom growth. Hierarchical clustering was performed based on growth-dependent variation patterns, and the results were presented as a dendrogram. Statistical

analyses were performed using the IBM SPSS Statistics version 28 (IBM Corp., Armonk, NY, USA).

2.3. Effect of wounding

The fruiting bodies of *P. cornucopiae* at the FB3 stage were used for the wounding experiments. Wounding was performed by cutting the fruiting bodies into approximately 5 mm wide pieces with scissors. The resulting tissue blocks were placed in 20 mL glass vials and incubated at either 25 °C or 4 °C with the caps tightly sealed. At each designated time point after wounding, 1 mL of methyl *tert*-butyl ether (MTBE) containing *n*-nonanyl acetate (1 μg mL^{-1}) was immediately added. The samples were thoroughly mixed to extract VOCs. The upper organic phase containing the extracted VOCs was collected after centrifugation at 120 × *g* for 10 min at 25 °C and subjected to GC–MS analysis. Three biological replicates ($n = 3$) were used for each time point.

Fruiting bodies at the FB1 stage (0.3 g) were cut into approximately 5 mm wide slices using scissors and placed into 2.0 mL screw-cap microcentrifuge tubes to examine changes in C8 VOC production in response to different degrees of tissue damage. One sample remained untreated. A second sample was rapidly frozen in liquid nitrogen and subsequently thawed in a 28 °C water bath for 10 min. A third sample was rapidly frozen in liquid nitrogen together with approximately 2 g of zirconia beads (0.5 mm diameter; YZB05; Yasui Kikai, Osaka, Japan) and mechanically disrupted using a bead crusher (Micro Smash MS-100R; TOMY Seiko, Tokyo, Japan) at 3500 rpm for 150 s, followed by thawing in a 28 °C water bath for 10 min. Four biological replicates ($n = 4$) were used for each treatment. To each tube, 500 μL of MTBE containing *n*-nonanyl acetate (1 μg mL^{-1}) was added. Samples were thoroughly mixed and centrifuged at 1680 × *g* for 2 min at 25 °C, and the resulting supernatants were subjected to GC–MS analysis. Microtome-cut sections were incubated in a 0.2% Tween 20 solution containing 5 mg mL^{-1} Evans blue (FUJIFILM Wako Pure Chemical) for 30 min to detect dead cells (Miyamoto et al., 2014). After incubation, sections were rinsed with water and observed under a light microscope (ECLIPSE Ni-U; Nikon, Tokyo, Japan).

Mycelia collected from the upper layer of the cultivation bed at the FCM stage were used to prepare the cell-free crude enzyme extract owing to their high activity in converting linoleic acid 10(*S*)-hydroperoxide (10(*S*)HPODE) to 1-octen-3-ol. Mycelia (ca. 0.3 g) were transferred to 2.0 mL screw-cap microtubes (SARSTEDT, Nümbrecht, Germany) and mixed with zirconia beads (0.5 mm diameter, 2.16 g) and 0.6 mL of 50 mM Tris–HCl buffer (pH 8.0). The samples were disrupted using a bead crusher at 4 °C and 3500 rpm for 2 min. The homogenates were centrifuged at 500 × *g* for 3 min at 4 °C, and the resulting supernatants were used as cell-free crude enzyme extracts. For the enzymatic reaction, 4 μL of the crude enzyme extract was mixed with 1 mL of 50 mM HEPES buffer (pH 7.0) containing 50 μM 10(*S*)HPODE. 10(*S*)HPODE was prepared using 10*S*-dioxygenase from the cyanobacterium *Nostoc punctiforme* as previously described (Teshima et al., 2022). The reaction mixture was incubated at 25 °C for 10 min. After incubation, 1 mL of MTBE containing *n*-nonanyl acetate (1 μg mL^{-1}) was immediately added, and the mixture was vortexed to extract VOCs. The samples were centrifuged at 112 × *g* for 10 min at 25 °C, and the organic phase was concentrated approximately fivefold under a nitrogen stream. The concentrated extracts were then subjected to gas chromatography-mass spectrometry (GC–MS).

GC-MS analysis was performed using the QP2010 Plus system (Shimadzu, Kyoto, Japan). Separation was achieved on a capillary column (DB-WAX, 30 m × 0.25 mm i.d., film thickness 0.25 μm; Agilent Technologies, Santa Clara, CA, USA). Helium was used as a carrier gas at a constant pressure of 61.8 kPa. The injector temperature was set to 240 °C, and samples were injected in splitless mode (sampling time, 2 min). The oven temperature program was as follows: 40 °C for 5 min; 40–200 °C at 5 °C min^{-1}; and 200 °C for 5 min. The mass spectrometer was operated in EI mode at 70 eV. The ion source and interface temperatures were set to 200 °C. Mass spectra were recorded in the *m/z* range of 35–350 in full-scan mode. 1-Octen-3-ol, 1-octen-3-one, and 3-octanone were quantified by comparison with calibration standards after normalizing their peak areas to those of the internal standard.

2.4. Feeding experiment

Fruiting bodies of *P. cornucopiae* at the FB3 stage were cut into cubes measuring approximately 1 cm. Tissue samples (200 mg) were placed in 20 mL glass vials, and 1 mL of 1-octen-3-ol, 1-octen-3-one, or 3-octanone solution was added. The solutions were prepared in 50 mM HEPES buffer (pH 7.0) containing 0.2% (w/v) Tween 20 at final concentrations of 50 or 100 μM. The vials were sealed tightly. After incubation at 25 °C for 30 min, 1 mL of MTBE containing *n*-nonanyl acetate (1 μg mL^{-1}) was added, and the mixture was thoroughly vortexed to extract VOCs. The extracted VOCs were analyzed using GC–MS as described above. The analysis was performed with four biological replicates ($n = 4$).

2.5. Proton-transfer reaction mass spectrometry

The PTR–MS system used in this study was a Custom Vocus 2R (Tofwerk AG, Thun, Switzerland), equipped with a discharge source generating H_3O^+ reagent ions, a focusing ion–molecule reactor (FIMR) operated at an electric field to number density ratio (E/N) of approximately 130 Td, a quadrupole ion guide, and a time-of-flight (ToF) mass analyzer with a mass resolving power of up to 11,000 at *m/z* 107 (full width at half maximum). VOCs were ionized by proton transfer from H_3O^+ reagent ions. The mass-resolving power was sufficient to determine the elemental composition of the detected ions and to resolve many isobaric species. The configurations of the discharge source and FIMR were identical to those previously described (Krechmer et al., 2018). Fruiting bodies at the FB2 stage were excised at the base using a razor blade and placed in an open-top glass container (6.7 cm i.d. × 6.7 cm height). Headspace VOCs were directly introduced into the PTR–MS inlet via a PTFE tube positioned near the fruiting bodies to monitor basal VOC emissions. After stabilization of the PTR–MS signals, the fruiting bodies were cut into approximately 5-mm-wide pieces using scissors while continuously introducing the emitted VOCs into the instrument. The inlet flow rate and time resolution were 0.1 L min^{-1} and 1 s, respectively. Mass spectral datasets were analyzed using Tofware (version 3.2.5; Tofwerk AG) implemented in Igor Pro (WaveMetrics, Lake Oswego, OR, USA).

A high-speed GC system was coupled with PTR–MS to analyze authentic standards and confirm that the fragment ions monitored by PTR–MS were specific to 1-octen-3-ol, 1-octen-3-one, and 3-octanone. GC separation was performed using a Sylph system (BallWave, Miyagi, Japan) equipped with a polyethylene glycol column (PEG20M; 30 m × 0.25 mm i.d., film thickness 0.25 μm). Hydrogen was used as the carrier gas at 1 mL min^{-1}. The oven temperature program was as follows: 50 °C for 5 min; 50–90 °C at 5 °C min^{-1}; and 90–180 °C at 10 °C min^{-1}, with a final hold at 180 °C for 3 min. The GC outlet was connected to the PTR–MS ion source via a glass capillary (0.53 mm i.d., 1.0 m length). For analysis of reference compounds, 1-octen-3-ol, 1-octen-3-one, and 3-octanone were introduced by mixing approximately 3.3 mL of room air containing vaporized analyte with 46.7 mL of ambient air (total volume 50 mL) (Ishihara et al., 2026). Similarly, VOCs emitted from wounded *P. cornucopiae* fruiting bodies were collected for 10 min (200 mL total volume), separated by high-speed GC, and subsequently analyzed using PTR, and were assigned to 1-octen-3-ol, 1-octen-3-one, and 3-octanone based on GC retention times.

2.6. Statistical analysis

VOC analyses other than the PTR–MS analysis were performed with three or four biological replicates. Data are presented as means ± standard error (SE). Statistical analyses were performed using

Excel Toukei (Bell Curve; SSRI Co. Ltd., Tokyo, Japan). The statistical methods are described in the respective figure legends.

3. Results

3.1. Developmental changes in VOCs in P. cornucopiae

When *P. cornucopiae* mycelia reached the edge of the MA plate, this stage was defined as the mycelium on the plate (MoP) stage and was used for inoculation onto the sawdust/rice-bran substrate (Fig. 1). After inoculation, the mycelia expanded to cover the surface of the cultivation bed and were designated as mycelia on mushroom bed (MoB) stage. The entire substrate was colonized within 14 days of inoculation. Basidiocarp formation was induced by opening the cultivation bag and exposing the fully colonized substrate to air; this stage was defined as the fully colonized mycelium (FCM) stage. Although a slight variation in timing was observed among the substrate batches, primordia appeared within 24–72 h of air exposure. The day on which the primordia were first detected was designated as fruiting body (FB) stage day 1 (FB1). Fruiting bodies typically reach a harvestable size 3 days after primordium formation (FB3). Thereafter, the caps expanded, the yellow coloration gradually faded, the tissues contracted, and the fruiting bodies turned brown by FB6. Spore release was most frequently observed between the FB3 and FB6 stages (Supplementary Fig. S2).

Under the present analytical conditions, C6–C10 aliphatic VOCs and sesquiterpenoids were detected as the major components (Fig. 2). Because sesquiterpene peaks were relatively small in the total ion chromatogram, extracted-ion chromatograms were generated using *m/z* 204 (corresponding to $C15H24^{+}$), which is characteristic of sesquiterpenes. The peak areas were calculated relative to the internal standard, and each compound was normalized to the maximum value observed during the monitoring period to visualize the temporal emission patterns. The normalized data are displayed as a heatmap, followed by hierarchical clustering and dendrogram construction (Figs. 3 and 4). The resulting clusters reflected growth-dependent production patterns spanning mycelial expansion, primordium induction, basidiocarp development, and senescence.

The C6–C10 aliphatic VOCs were further classified into four clusters (Fig. 3A; Groups A–D). Group A comprised 1-octen-3-ol, 1-octen-3-one, and 3-octanone. These compounds were present at low levels during the mycelial stage. However, their production increased sharply upon bag opening (FCM) and decreased rapidly with FB1. From FCM onward, Group A compounds consistently exhibited higher abundances in the morning and lower abundances in the afternoon. Among these, 3-octanone was the most abundant. Group B consisted of hexanoic acid and octanoic acid, both of which peaked at FB2 prior to intensive spore release. Group C included 3-heptanone, hexanal, nonanal, and related compounds. These VOCs were abundant during the mycelial growth stage and remained detectable after fruiting induction; however, their levels declined markedly from FB3 onward. Group D included 3-methylbutanoic acid and pentylpropionate. Production of these compounds was suppressed during mycelial colonization but remained relatively constant from FB0 (the day primordia became evident) through the main spore release period (FB4–FB5) and persisted until FB6. Among the detected VOCs, 3-octanone and 1-octen-3-ol were the most abundant following fruiting induction. The emission rates were quantified using authentic standards (Fig. 3B). Emission of 3-octanone peaked at the fully colonized bed (FCM) stage, when the substrate was fully colonized and exposed to air, with an emission rate of 230 μg per bed per hour. Similarly, 1-octen-3-ol emission peaked at the FCM stage, reaching 8.5 μg per bed per hour.

Hierarchical clustering and dendrogram analysis classified the sesquiterpenes into three groups (E–G) (Fig. 4). Group E comprised nine compounds, with α-muurolene as the most abundant. These compounds were scarcely detected during the mycelial stages and from primordium formation through early fruiting body development; however, their abundance increased with the onset of spore release and continued to increase during senescence, reaching a maximum at FB6. Group F included sesquiterpene (3) and cadinene. The emissions of these compounds peaked during primordium formation and subsequently declined. In contrast, Group G consisted solely of α-cedrene, which was mostly detected during the FCM stages.

3.2. VOC formation upon tissue damage

Rapid VOC formation following tissue damage has been reported in the fruiting bodies of several basidiomycete species (Combet et al., 2009; Spiteller, 2008). Such responses may have ecological significance, and may contribute to flavor changes during the processing of edible mushrooms. FB3 fruiting bodies (at the onset of spore release)

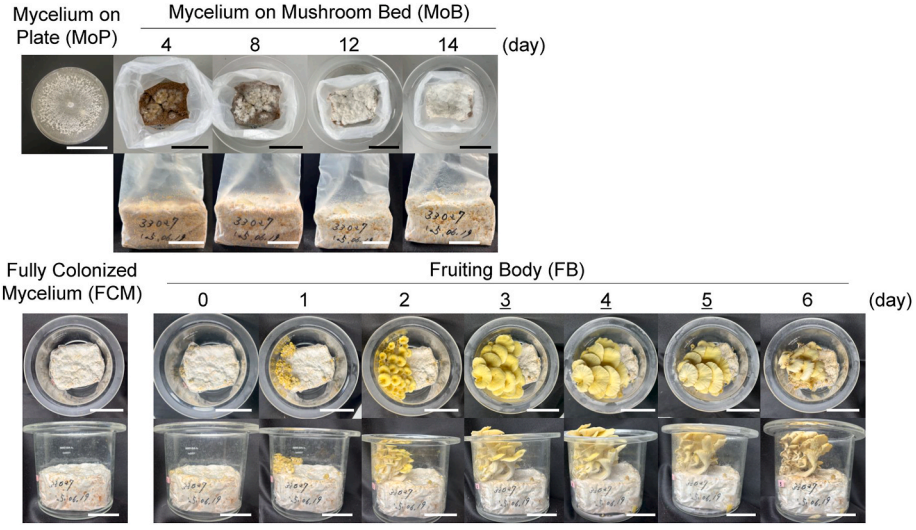

Fig. 1. Developmental stages of *Pleurotus cornucopiae* used for VOC sampling. Mycelia grown on MA plates (mycelia on plates, MoP) were inoculated onto a sawdust–rice bran substrate, sealed in polyethylene bags, and incubated for 14 days (mycelia on bed, MoB). The plastic bag was then opened for overhead photography. The upper portion of the bag was removed to induce primordium formation when the substrate was fully colonized (fully colonized mycelium, FCM). The day on which distinct primordia were first observed was designated as day 0, and fruiting bodies (FB) were sampled for up to 6 days thereafter until senescence. Scale bar, 5 cm.

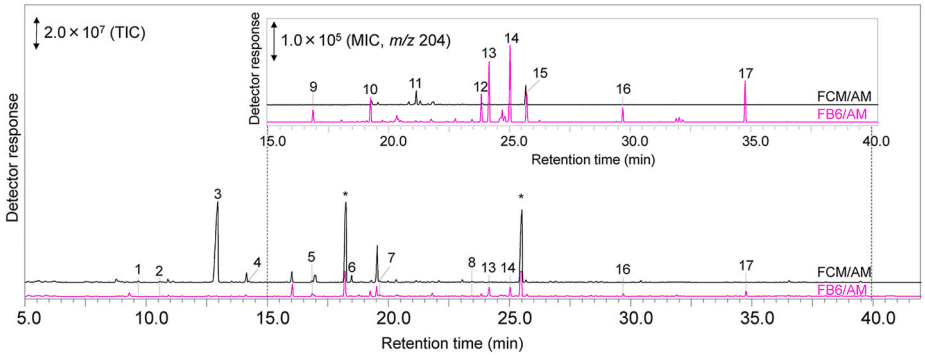

Fig. 2. Representative GC–MS chromatograms of volatile compounds emitted from *P. cornucopiae*. Results obtained at the fully colonized mycelium (FCM) stage and six days after fruiting body formation (FB6) stage are shown. The inset shows the extracted ion chromatogram at *m/z* 204. Peak 1: 3-heptanone, 2: heptanol, 3: 3-octanone, 4: 1-octen-3-one, 5: nonanol, 6: 1-octen-3-ol, 7: decanal, 8: 3-methylbutanoic acid, 9: sesquiterpene (2), 10: α-copaene, 11: α-cedrene, 12: sesquiterpene (1), 13: γ-muurolene, 14: α-muurolene, 15: δ-cadinene, 16: cubelol, 17: α-cadinol. Peaks marked with an asterisk (*) indicate contaminant compounds originating from the container or the surrounding environment.

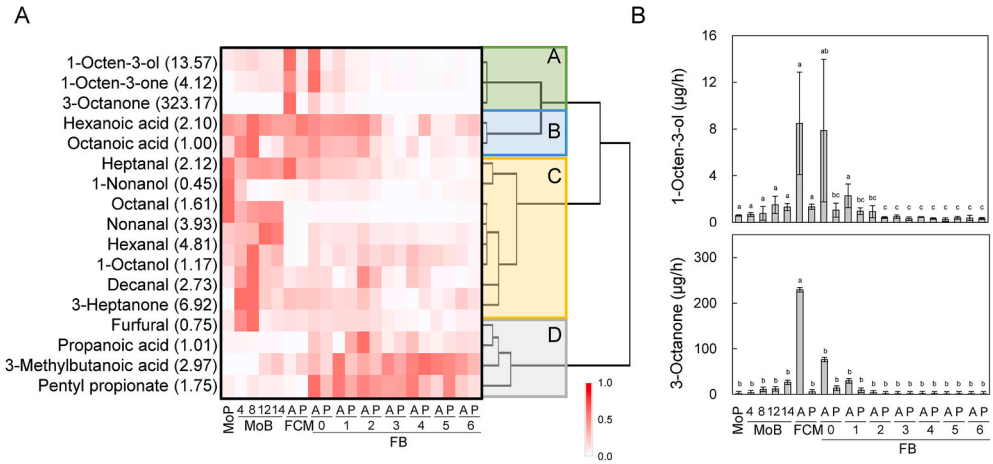

Fig. 3. Developmental changes in volatile compounds putatively derived from fatty acids and amino acids in *P. cornucopiae*. (A) Heatmap showing GC–MS peak area ratios relative to the internal standard. Numbers in parentheses indicate the maximum peak area ratio observed for each compound. Hierarchical clustering based on developmental emission patterns is presented as a dendrogram; compounds were classified into Groups A–D accordingly. (B) Quantification of C8 volatile compounds using authentic standards. Data are means ± SE. Statistical significance was determined by one-way ANOVA followed by Tukey's HSD test; different letters indicate significant differences at $P < 0.05$. In the x-axis labels, A and P indicate morning (9:30–11:00) and afternoon (15:30–17:00) sampling, respectively.

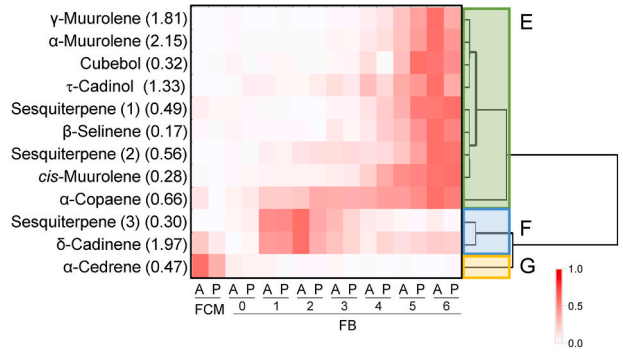

Fig. 4. Developmental changes in sesquiterpene volatiles emitted from *P. cornucopiae*. Heatmap showing GC–MS peak area ratios relative to the internal standard. Numbers in parentheses indicate the maximum peak area ratios observed for each compound. Hierarchical clustering based on developmental emission patterns was presented as a dendrogram, and compounds were classified into Groups E–G. In the x-axis labels, A and P indicate morning (9:30–11:00) and afternoon (15:30–17:00) sampling, respectively.

were sectioned into 5 mm slices to examine damage-induced VOC production. VOCs formed immediately before cutting and 60 min after cutting were extracted and analyzed using GC–MS (Fig. 5).

The major VOCs detected in sliced fruiting bodies were 3-octanone, 1-octen-3-ol, and 1-octen-3-one, whereas sesquiterpenes were rarely detected. Substantial increases in all three compounds were observed as early as 1 min after wounding. In contrast, their levels remained low in intact fruiting bodies, indicating rapid *de novo* formation upon tissue damage. Both 1-octen-3-one and 1-octen-3-ol reached their maximum levels within 1 min, returned to basal levels within 5 min, and remained at low levels for 60 min. 1-Octen-3-ol accumulated to approximately six-fold higher levels than 1-octen-3-one. In contrast, 3-octanone formation peaked at 5 min after wounding, reaching 700 ng g^{-1}, and subsequently declined more gradually over the following 60 min than 1-octen-3-one and 1-octen-3-ol. These wound-induced kinetic differences among C8 VOCs were more clearly resolved at low temperatures. At 4 °C, 1-octen-3-one and 1-octen-3-ol reached their maxima at 40–90 s after wounding and then decreased gradually until 10 min post-wounding. In contrast, the 3-octanone concentration continued to increase for up to 10 min (Supplementary Fig. S3).

Intact *P. cornucopiae* fruiting bodies at the FCM stage (morning sampling) emitted 3-octanone at 8.5 μg h^{-1} and 1-octen-3-ol at 0.23 μg h^{-1} (Fig. 3B), corresponding to a production ratio of approximately 40. In contrast, partial wounding by slicing of the fruiting bodies

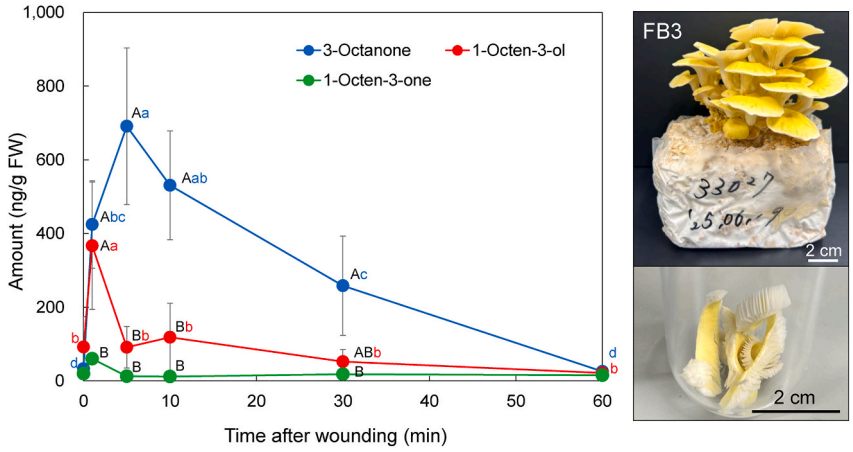

Fig. 5. Wound-induced formation of C8 volatile compounds in fruiting bodies of *P. cornucopiae*. Fruiting bodies at the FB3 stage were cut, and C8 VOCs generated at defined time intervals were extracted with an organic solvent and analyzed using GC–MS. The developmental stage of the fruiting bodies used, along with representative images after cutting, is shown on the right.

resulted in the formation of nearly equal amounts of the two compounds. For example, 1 min after cutting, 3-octanone and 1-octen-3-ol were detected at concentrations of 424 and 367 ng g^{-1}, respectively (Fig. 5). Based on previous observations of *Agaricus bisporus* fruiting bodies (Combet et al., 2009), we hypothesized that the production ratio of 3-octanone to 1-octen-3-ol depends on tissue integrity. To test this hypothesis, FB1-stage fruiting bodies were analyzed under three conditions: (i) intact tissue, (ii) tissue subjected to freeze–thaw treatment to induce partial cellular disruption, and (iii) tissue completely homogenized with zirconia beads following freeze–thaw treatment. The amounts of 3-octanone and 1-octen-3-ol produced under each condition were compared (Fig. 6). Evans blue staining revealed that only a limited number of cells on the cut surfaces stained blue, whereas the number of Evans blue–positive cells markedly increased after freeze–thaw treatment. Under these experimental conditions, the ratio of 3-octanone to 1-octen-3-ol in sliced tissues was 16.7; this ratio decreased to 2.60 after freeze–thaw treatment, and further to 0.63 following complete homogenization. Although the total amounts of 3-octanone and 1-octen-3-ol produced increased only modestly (1.72, 1.87, and 2.05 μg g^{-1} for intact, freeze–thaw–treated, and homogenized tissues, respectively), the relative production ratio of these two C8 VOCs varied substantially depending on the degree of tissue disruption. The rapid formation of C8 VOCs was suppressed when freeze-thaw treatment was carried out under anaerobic conditions (Supplementary Fig. S4).

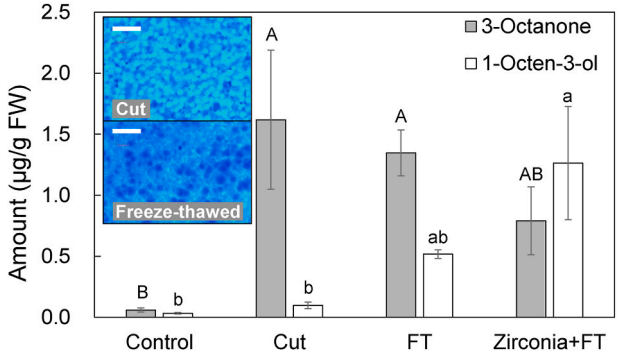

Fig. 6. Effect of wounding severity on the production of 3-octanone and 1-octen-3-ol. Fruiting bodies at stage FB4 were left intact (control), cut into 5-mm slices (Cut), subjected to freeze–thaw treatment (FT), or completely homogenized with zirconia beads following freeze–thaw treatment (Zirconia + FT). VOCs produced under each condition were extracted and quantified. Values are presented as means ± standard error (SE) ($n = 4$). Statistical analysis was performed using one-way ANOVA followed by Tukey's HSD test. Different uppercase letters indicate significant differences in 3-octanone levels, and different lowercase letters indicate significant differences in 1-octen-3-ol levels ($P < 0.05$). Inset images (upper left) show representative Evans blue staining of Cut and FT fruiting bodies, highlighting dead cells. Scale bar, 20 μm. (For interpretation of the references to color in this figure legend, the reader is referred to the Web version of this article.)

When a cell-free crude enzyme extract prepared from the primordia was incubated with 10(*S*)-HPODE, 1-octen-3-ol and 1-octen-3-one were detected, whereas 3-octanone was barely detectable (Supplementary Fig. S5). The amount of 1-octen-3-one did not differ between the reactions containing the untreated crude enzyme extract and those lacking the crude enzyme extract, or those containing heat-denatured crude enzyme extract (Supplementary Fig. S5). Although appreciable amounts of 1-octen-3-ol were detected in reactions lacking the crude enzyme extract or containing the heat-denatured crude enzyme extract, its production was significantly higher in the presence of the untreated crude enzyme extract. Because 10(*S*)-HPODE is susceptible to thermal decomposition, yielding 1-octen-3-ol and 1-octen-3-one as the major products (Miyazaki et al., 2023), it is likely that 10(*S*)-HPODE underwent partial thermal degradation during extraction and GC analysis. After correcting for this non-enzymatic formation, the cell-free crude enzyme preparation can be regarded as exclusively producing 1-octen-3-ol.

3.3. PTR-ToF-MS analysis

PTR-MS enables non-invasive, near-real-time analysis of VOC production and is therefore useful for investigating the dynamics of VOC generation in response to various stimuli applied to biological samples (Majchrzak et al., 2020; Tholl et al., 2021). We conducted real-time VOC monitoring using PTR–ToF–MS (Fig. 7) to gain mechanistic insights into the relationships among wound-induced C8 VOCs in *P. cornucopiae* and examine the time-course patterns observed in Fig. 5 with a much higher temporal resolution. A fruiting body that was carefully excised from the substrate was placed in a glass container, and a PTR–MS inlet tube was positioned inside the container to monitor the VOCs emitted from the intact tissue. C8 compounds were identified as dominant VOCs. The assignments of the individual C8 compounds were confirmed by comparison with authentic standards using the Sylph GC–PTR–ToF–MS system (Supplementary Fig. S6) (Ishihara et al., 2026).

Cutting the fruiting body inside a glass container immediately triggers C8 formation. Signals corresponding to $C_8H_{15}^+$ (associated with 1-octen-3-ol) and $C_8H_{15}O^+$ (associated with 1-octen-3-one) increased within 1 s after wounding, reached maxima at 8–12 s, and subsequently decayed. Notably, the production kinetics of 1-octen-3-ol and 1-octen-3-

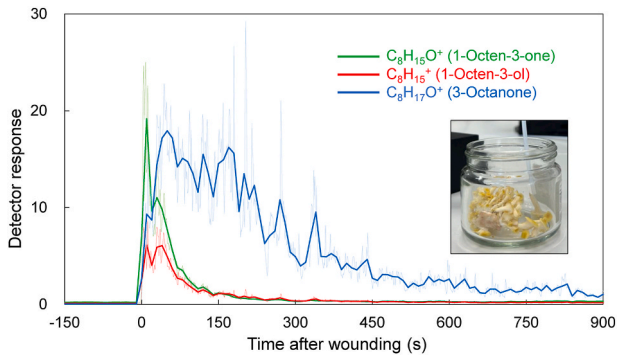

Fig. 7. Real-time PTR–ToF–MS analysis of C8 VOCs emitted from wounded fruiting bodies of *P. cornucopiae*. The fruiting bodies at the FB2 stage were excised with minimal mechanical damage and placed in a glass container. A PTFE tube connected to the PTR–ToF–MS inlet was positioned at the center of the container, and VOC monitoring was initiated. After signal stabilization (>5 min), the fruiting bodies were cut inside the container (time 0), with continuous monitoring maintained. Ions $C_8H_{17}O^+$, $C_8H_{15}^+$, and $C_8H_{15}O^+$ were monitored as the characteristic fragment ions of 3-octanone, 1-octen-3-ol, and 1-octen-3-one, respectively. Pale traces indicate raw data acquired at 1-s intervals; dark traces represent data smoothed over 10-s intervals. This figure shows a representative time course obtained from one experiment. Another independent experiment showing a similar temporal response is presented in Supplementary Fig. S7.

one were nearly identical, even at the second-scale resolution. In contrast, the $C_8H_{17}O^+$ signal (associated with 3-octanone) also increased from 1 s after wounding but peaked later, at 44 s. The emission of 3-octanone then declined more gradually than those of 1-octen-3-ol and 1-octen-3-one. A similar time-course profile was observed in an independent analysis performed on a different day (Supplementary Fig. S7). The overall temporal patterns observed by PTR–MS are consistent with the quantitative GC–MS results shown in Fig. 5. The ion associated with sesquiterpenes ($C_{15}H_{25}^+$; m/z 205.196) exhibited only a transient increase immediately after cutting and rapidly returned to basal levels (Supplementary Fig. S8).

To further investigate the biosynthetic relationships among C8 VOCs, blocks of *P. cornucopiae* fruiting bodies were immersed in solutions containing 1-octen-3-ol, 1-octen-3-one, or 3-octanone. After 30 min of incubation, C8 VOCs were extracted and quantified (Fig. 8). Feeding

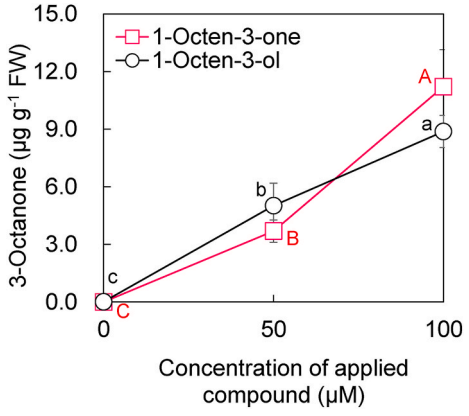

Fig. 8. Concentration-dependent formation of 3-octanone following application of 1-octen-3-ol (circle) or 1-octen-3-one (square) to fruiting body blocks. Values are presented as means ± standard error (SE) ($n = 4$). Statistical analysis was performed using one-way ANOVA followed by Tukey's HSD test. Different uppercase letters indicate significant differences in 3-octanone levels among dose-dependent treatments with 1-octen-3-one, whereas different lowercase letters indicate significant differences among dose-dependent treatments with 1-octen-3-ol ($P < 0.05$).

with 1-octen-3-ol resulted in concentration-dependent formation of 3-octanone, whereas the production of 1-octen-3-one was negligible. Similarly, feeding 1-octen-3-one led to the concentration-dependent formation of 3-octanone; however, no production of 1-octen-3-ol was detected under these conditions. In contrast, treatment with 3-octanone hardly altered the 1-octen-3-ol or 1-octen-3-one levels.

4. Discussion

By characterizing VOCs emitted during mushroom development and after mechanical wounding, we aimed to provide a basis for understanding the physiological and ecological significance of fungal VOC emissions. Analyses of developing mushrooms revealed diverse aliphatic VOCs and sesquiterpenes with distinct developmental patterns. Among the aliphatic VOCs, group A C8 VOCs were predominant, whereas most sesquiterpenes belonged to group E. Therefore, we focused on these major VOCs, which show clear developmental regulation, in the present study. Aliphatic VOCs in groups B–D also exhibited characteristic developmental changes. Although compounds such as hexanoic acid and hexanal have been reported in fungi (Lemfack et al., 2018; the mVOC database is available at http://bioinformatics.charite.de/mvoc), little is known about their biosynthesis and physiological roles. Various sesquiterpenes have also been reported in basidiomycetes and some of their biosynthetic enzymes have been identified; however, little is known about their physiological and ecological functions (Wu et al., 2022). Further studies on the biosynthetic pathways and the physiological and ecological functions of these compounds are important for a comprehensive understanding of mushroom VOC production.

Although most fungi rely primarily on wind for spore dispersal, some species also depend, at least in part, on fungivores for this process (Kimura and Tuno, 2024). Spores can be transported by attachment to the body surface of fungivores or by ingestion together with the fruiting body, followed by retention in the digestive tract and dispersal across the animal's movement range (Kobayashi et al., 2017; Santana and Couceiro, 2024). Analogous to the interactions between angiosperms and pollinators, VOCs have been proposed as potential cues for attracting fungivores (Santamaria et al., 2023; Yin et al., 2025). In our dataset, VOCs belonging to the sesquiterpene Group E increased markedly from FB4 to FB6, a developmental stage that follows the onset of spore release. Spores of *Pleurotus djamor* reportedly retain some germination ability after passing through the digestive tract of mycophagous *Drosophila angularis* (Kobayashi et al., 2017). *P. cornucopiae* is preyed upon in the field by members of the Drosophilidae and Mycetophilidae (Kimura and Toda, 1989; Ševčík, 2006). Many of these fungivores exhibit host specificity, and some species, such as *Drosophila testacea*, are more frequently found on decaying fruiting bodies of *P. cornucopiae* than on fresh ones (Kimura and Toda, 1989). β-Guaiene and δ/γ-cadinene emitted by the polypore basidiomycete, *Trametes versicolor*, elicit antennal responses in beetles such as *Diaperis boleti* (Drilling and Dettner, 2009). Whether the increased emission of Group E sesquiterpenes contributes to interactions with these fungivores remains unknown; at present, there is no direct evidence that *P. cornucopiae* emits VOCs to attract fungivores, thereby benefiting from enhanced spore dispersal. Future field studies on spore dispersal, together with behavioral assays (e.g., olfactometer tests) and electrophysiological analyses (e.g., GC–electroantennography), will be important for determining whether Group E sesquiterpenes contribute to interactions between *P. cornucopiae* and fungivores.

In contrast, C8 VOCs were released in large amounts during the early reproductive stage and were also emitted rapidly and abundantly following tissue damage. Their ecological roles may be linked to their distinct emission patterns. Several *Pleurotus* species, including *P. ostreatus*, form small lollipop-shaped structures on hyphae that accumulate 3-octanone; this 3-octanone can paralyze and kill nematodes (Barron and Thorn, 1987; Lee et al., 2023). In the ascomycete *Podospora anserina*, loss of 1-octen-3-ol production reduces the efficiency of

nematode repulsion (Ferrari et al., 2018). Furthermore, VOCs produced by *Aspergillus fumigatus* are toxic to *Drosophila melanogaster* larvae, and their toxicity is reduced in a 1-octen-3-ol-deficient strain (Almaliki et al., 2023). Olfactometer bioassays have shown that the fungivorous beetle *Bolitophagus reticulatus* prefers 3-octanone but avoids 1-octen-3-ol (Holighaus et al., 2014). In contrast, the fungivorous ladybird beetle *Psyllobora vigintimaculata* prefers 1-octen-3-ol and is unresponsive to 3-octanone (Tabata et al., 2011). Although these studies suggest that C8 VOCs can influence the interactions between fungi and invertebrates in diverse ways, their ecological functions in *P. cornucopiae* remain unknown. Identifying the fungivores that interact with *P. cornucopiae* under natural conditions, together with detailed analyses of their behavioral responses to mushroom VOCs, will be important for clarifying the ecological roles of C8 VOCs. In addition to their effects on invertebrates, C8 VOCs at high concentrations are known to inhibit fungal spore germination and induce mycotoxin accumulation. In plants, they can suppress seed germination and trigger defense responses (Pennerman et al., 2022). Therefore, it is important to consider the ecological significance of C8 VOC production in basidiomycetes in terms of its effects on microorganisms and plants.

The C8 VOCs bearing an oxygen atom at the C3 position—3-octanone, 1-octen-3-ol, and 1-octen-3-one [C8 VOCs consisting of 'ketonic-cycle' (Karrer et al., 2021)]—are rapidly produced upon wounding of most basidiomycete fruiting bodies (Spiteller, 2008). In *P. cornucopiae* fruiting bodies, slicing immediately triggered the formation of 1-octen-3-ol, 1-octen-3-one, and 3-octanone. Because these compounds are present at much lower levels in intact fruiting bodies, their rapid increase reflects *de novo* synthesis. PTR-ToF-MS analysis revealed pronounced increases in all three C8 VOCs within 1 s after slicing, which is consistent with the near-instant activation of the biosynthetic machinery upon tissue damage. Based on available evidence, 1-octen-3-ol is most likely the first C8 VOC to be biosynthesized. The rapid accumulation of 1-octen-3-ol in wounded fruiting bodies is presumably due to the immediate activation, in damaged tissues, of dioxygenase-mediated conversion of linoleic acid to 10(*S*)HPODE followed by a subsequent cleavage reaction. Although 1-octen-3-ol was also produced upon freeze–thaw treatment of fruiting bodies, its formation was effectively suppressed when the tissues were thawed under anaerobic conditions (Supplementary Fig. S4). These observations indicated that the production of 1-octen-3-ol in wounded tissues was primarily regulated during oxygenation.

The biosynthetic sequence of C8 VOC in basidiomycetes has not yet been fully elucidated (Karrer et al., 2021). This study demonstrated that the production of 1-octen-3-ol and 1-octen-3-one was tightly synchronized, whereas the production of 3-octanone was clearly delayed. A cell-free enzyme assay showed that 1-octen-3-ol is enzymatically formed from 10(*S*)-HPODE, whereas 1-octen-3-one may be formed, at least in part, through the non-enzymatic decomposition of 10(*S*)-HPODE. Feeding experiments using sliced fruiting bodies showed that supplementation with 1-octen-3-ol or 1-octen-3-one resulted in the formation of 3-octanone. Moreover, a comparison of C8 VOC production among sliced, freeze–thaw-treated, and completely disrupted tissues suggested that 3-octanone formation requires intact tissues. Similar to wound-induced GLV biosynthesis in angiosperms (Matsui et al., 2012), it is possible that 1-octen-3-ol and/or 1-octen-3-one produced in damaged cells diffuses into adjacent intact cells, where they are subsequently converted into 3-octanone. To verify this hypothesis, we identified the enzyme(s) responsible for converting 1-octen-3-ol and/or 1-octen-3-one into 3-octanone.

To elucidate the physiological and ecological functions of fungal VOCs, future studies should focus on identifying the enzymes involved in their biosynthesis and the genes that encode them. Targeted disruption of these genes, combined with analyses of fruiting body development and the responses and performance of interacting organisms, is essential for clarifying the roles of these VOCs in fungal physiology and ecology.

Declaration of generative AI and AI-assisted technologies in the manuscript preparation process

During the preparation of this work, the author(s) used ChatGPT to improve English. After using this tool/service, the author(s) reviewed and edited the content as needed and take(s) full responsibility for the content of the published article.

Funding sources

This work was financially supported by JSPS KAKENHI Grant Number 23K26833 and 26H01133.

CRediT authorship contribution statement

Yuki Nagata: Conceptualization, Investigation, Methodology, Writing – original draft. **Kozue Sotome:** Methodology, Resources, Writing – review & editing. **Daisuke Fukuyama:** Investigation, Methodology, Writing – review & editing. **Kanako Sekimoto:** Investigation, Methodology, Software, Writing – review & editing. **Kenji Matsui:** Conceptualization, Funding acquisition, Project administration, Supervision, Writing – original draft, Writing – review & editing.

Declaration of competing interest

The authors declare that they have no known competing financial interests or personal relationships that could have appeared to influence the work reported in this paper.

Acknowledgments

The authors thank the Fungus/Mushroom Resource and Research Center (FMRC) at the Tottori University Fungal Culture (TUFC) with support from the National BioResource Project of MEXT, Japan, for providing the mushroom resources used in this study.

Appendix A. Supplementary data

Supplementary data to this article can be found online at https://doi.org/10.1016/j.funbio.2026.101824.

References

Almaliki, H.S., Niu, M., Keller, N.P., Yin, G., Bennett, J.W., 2023. Mutational analysis of *Aspergillus fumigatus* volatile oxylipins. J. Fungi 9, 402.
Aprea, E., Romano, A., Betta, E., et al., 2015. Volatile compound changes during shelf life of dried *Boletus edulis*: Comparison between SPME-GC-MS and PTR-ToF-MS analysis. J. Mass Spectrom. 50, 56–64.
Barron, G.L., Thorn, R.G., 1987. Destruction of nematodes by *Pleurotus* species. Can. J. Bot. 65, 774–778.
Chang, C.H., Urban, P.L., 2018. Automated dual-chamber sampling system to follow dynamics of volatile organic compounds emitted by biological specimens. Anal. Chem. 90, 13848–13854.
Combet, E., Henderson, J., Eastwood, D.C., Burton, K.S., 2009. Influence of sporophore development, damage, storage, and tissue specificity on the enzymic formation of volatiles in mushrooms (Agaricus bisporus). J. Agric. Food Chem. 57, 3709–3717.
D'Auria, J.C., Pichersky, E., Schaub, A., Hansel, A., Gershenzon, J., 2007. Characterization of a BAHD acyltransferase responsible for producing the green leaf volatile (*Z*)-3-hexen-1-yl acetate in Arabidopsis thaliana. Plant J. 49, 194–207.
Drilling, K., Dettner, K., 2009. Electrophysiological responses of fungivorous coleoptera. Chemoecology 19, 109–115.
Ševčík, J., 2006. Diptera associated with fungi in the Czech Republic and Slovakia. Čas. Slez. Muz. Opava (A) 55, 1–84.
Ferrari, R., Lacaze, I., Le Faouder, P., et al., 2018. Fungal cyclooxygenases and lipoxygenases repel nematodes. Biochim. Biophys. Acta Gen. Subj. 1862, 2174–2182.
Fäldt, J., Jonsell, M., Nordlander, G., et al., 1999. Volatiles of bracket fungi Fomitopsis pinicola and Fomes fomentarius and their functions as insect attractants. J. Chem. Ecol. 25, 567–590.
Holighaus, G., Weißbecker, B., von Fragstein, M., et al., 2014. Eight-carbon volatiles as infochemicals. Chemoecology 24, 57–66.
Inamdar, A.A., Morath, S., Bennett, J.W., 2020. Fungal volatile organic compounds: more than just a funky smell? Annu. Rev. Microbiol. 74, 101–116.

Ishihara, R., Fukuyama, D., Sekimoto, K., 2026. Interpretation of α-pinene mass spectra using APCDI. Mass Spectrom. 15, A0190.
Karrer, D., Weigel, V., Hoberg, N., et al., 2021. C8-oxylipin biosynthesis in *Cyclocybe aegerita*. Mycol. Prog. 20, 929–940.
Kimura, M.T., Toda, M.J., 1989. Food preferences and nematode parasitism in mycophagous Drosophila. Ecol. Res. 4, 209–218.
Kimura, M.T., Tuno, N., 2024. Phylogeny, ecology, and evolution of mycophagous Drosophilidae. Biol. J. Linn. Soc. 142, 247–260.
Kobayashi, M., Kitabayashi, K., Tuno, M., 2017. Spore dissemination by mycophagous drosophilids. Ecol. Res. 32, 621–626.
Krechmer, J., Lopez-Hilfiker, F., Koss, A., et al., 2018. Evaluation of a new reagent-ion source for PTR-MS. Anal. Chem. 90, 12011–12018.
Lee, C.H., Lee, Y.Y., Chang, Y.C., et al., 2023. A carnivorous mushroom kills nematodes via a volatile ketone. Sci. Adv. 9, eade4809.
Lemfack, M.C., Gohlke, B.O., Toguem, S.M.T., Preissner, S., Piechulla, B., Preissner, R., 2018. mVOC 2.0: a database of microbial volatiles. Nucleic Acids Res. 46, D1261–D1265.
Majchrzak, T., Wojnowski, W., Wasik, A., 2020. Proton transfer reaction mass spectrometry for plant metabolomics. Trends Plant Sci. 25, 313–314.
Matsui, K., Sugimoto, K., Mano, J., Ozawa, R., Takabayashi, J., 2012. Differential metabolisms of green leaf volatiles in injured and intact parts of a wounded leaf meet distinct ecophysiological requirements. PLoS One 7, e36433.
Matsui, N., Ohira, T., Hiramatsu, Y., et al., 2007. Composition of volatiles from tatami mats containing hinoki (*Chamaecyparis obtusa*) wood wool. J. Wood Sci. 53, 529–532.
Miyamoto, K., Murakami, T., Kakumyan, P., Keller, N.P., Matsui, K., 2014. Formation of 1-octen-3-ol from Aspergillus flavus conidia after cell disruption. PeerJ 2, e395.
Miyazaki, R., Kato, S., Otoki, Y., et al., 2023. Decomposition pathways of linoleic acid hydroperoxide isomers. Biosci. Biotechnol. Biochem. 87, 179–190.
Orban, A., Hennicke, F., Rühl, M., 2020. Volatilomes of *Cyclocybe aegerita* during different stages of monokaryotic and dikaryotic fruiting. Biol. Chem. 401, 995–1004.
Orban, A., Schwab, L.J., Lugones, L.G., et al., 2023. Effect of fruiting-related genes on the formation of volatile organic compounds in the mushroom *Schizophyllum commune*. Mycol. Prog. 22, 67.
Pennerman, K.K., Yin, G., Bennett, J.W., 2022. Eight-carbon volatiles: prominent fungal and plant interaction compounds. J. Exp. Bot. 73, 487–497.
Santamaria, B., Verbeken, A., Haelewaters, D., 2023. Mycophagy: a global review. J. Fungi 9, 163.
Santana, M.D.F., Couceiro, S.R.M., 2024. Spore dispersal of *Phallus indusiatus* s. l. Food Webs. 38, e00338.
Sato, M., Torigoe, D., Kinoshita, Y., et al., 2025. Long-term intake of Tamogi-take mushroom (*Pleurotus cornucopiae*) mitigates age-related cardiovascular dysfunction. NPJ Aging 11, 1.
Spiteller, P., 2008. Chemical defence strategies of higher fungi. Chemistry 14, 9100–9110.
Tabata, J., De Moraes, C.M., Mescher, M.C., 2011. Olfactory cues from mildew-infected plants. PLoS One 6, e23799.
Teshima, T., Funai, R., Nakazawa, T., et al., 2022. *Coprinopsis cinerea* dioxygenase essential for 1-octen-3-ol synthesis. J. Biol. Chem. 298, 102507.
Tholl, D., Hossain, O., Weinhold, A., Röse, U.S.R., Wei, Q., 2021. Trends and applications in plant volatile sampling and analysis. Plant J. 106, 314–325.
Veerabahu, A., Banik, M.T., Lindner, D.L., Pringle, A., Jusino, M.A., 2025. Invasive golden oyster mushrooms disrupt native fungal communities across North America. Curr. Biol. 35, 3994–4002.
Wang, Q., Cao, R., Zhang, Y., Qi, P., Wang, L., Fang, S., 2021. Biosynthesis and regulation of terpenoids from basidiomycetes: exploration of new research. AMB Express 11, 150.
Wu, J., Yang, X., Duan, Y., Wang, P., Qi, J., Gao, J.-M., Liu, C., 2022. Biosynthesis of sesquiterpenes in aasidiomycetes: a review. J. Fungi 8, 913.
Wurzenberger, M., Grosch, W., 1984. Formation of 1-octen-3-ol from the 10-hydroperoxide isomer of linoleic acid by a hydroperoxide lyase in mushrooms (*Psalliota bispora*). Biochim. Biophys. Acta 794, 25–30.
Yin, G., Moore, G.G., Bennett, J.W., 2025. Diversity and functions of fungal VOCs. Mycology 16, 1011–1022.